Raman evidence of a new high-pressure phase in calcium hydride

2007 J. Phys.: Condens. Matter 19 226205

(http://iopscience.iop.org/0953-8984/19/22/226205)

IOP PUBLISHING JOURNAL OF PHYSICS: CONDENSED MATTER

J. Phys.: Condens. Matter **19** (2007) 226205 (7pp) doi:10.1088/0953-8984/19/22/226205

Raman evidence of a new high-pressure phase in calcium hydride

Bing Li, Yinwei Li, Kaifeng Yang, Qiliang Cui, Yanming Ma[1] and Guangtian Zou[1]

National Laboratory of Superhard Materials, Jilin University, Changchun 130012, People's Republic of China

E-mail: mym@jlu.edu.cn and gtzou@jlu.edu.cn

Received 6 February 2007, in final form 10 April 2007
Published 3 May 2007
Online at stacks.iop.org/JPhysCM/19/226205

Abstract

A new high-pressure phase of solid calcium hydride at room temperature was discovered by *in situ* Raman scattering experiments with a diamond anvil cell. The phase transition was found to start at ∼15.5 GPa and complete at ∼21 GPa, and it is reversible with a hysteresis to ∼12 GPa, when the pressure was released. Moreover, the high-pressure phase was found to be stable up to at least 42 GPa. First-principles calculations were performed to assign the measured Raman modes at zero pressure accurately and to understand the pressure dependence of the Raman frequency shift before the transition.

(Some figures in this article are in colour only in the electronic version)

Metal hydrides are of great scientific and technological interest in view of their potential applications for hydrogen storage [1], and are also of fundamental importance because of their intriguing electronic, structural, and dynamical properties associated with the hydrogen atoms. In particular, those metal hydrides with high hydrogen-to-metal ratio, such as the group II hydrides (MgH_2, CaH_2, SrH_2, and BaH_2), are desirable for real applications. The utilization of high-pressure technology has made considerable progress in experimental studies of hydrogen storage materials. It has been demonstrated that the application of high pressure is an effective tool for producing vacancies in the host metallic matrix for a number of metal–hydrogen systems, which in turn leads to various novel properties [2]. Also, it has recently been established that improved hydrogen absorption kinetics can be achieved by reducing the particle size to magnesium hydrides [3]. Therefore, in order to improve the hydrogen storage properties of metals or metal alloys, an understanding of the structural stability and bonding nature of metal hydrides is considered to be essential.

[1] Address for correspondence: National Lab of Superhard Material, Jilin University, 2699 Qianjin Street, 130012, Changchun, People's Republic of China.

At ambient conditions, in group II hydrides, MgH_2 has a rutile-type structure (α-MgH_2) with the space group $P4_2/mnm$, while CaH_2, SrH_2 and BaH_2 adopt an orthorhombic structure with the space group *Pnma* [4]. The high-pressure behaviour of MgH_2 has been studied extensively by using first-principles simulations [5], x-ray diffraction measurement [6, 7], and their combination [6]. Although the pressure-induced structural phase transition sequence of MgH_2 under high pressure is still under debate, it is clear that new structural modifications (such as *Pbcn* and *Pbca* phases, etc) form under pressure. However, there have been no reports on high-pressure research on CaH_2, SrH_2 and BaH_2 in the literature. In this letter, we present *in situ* Raman scattering measurements on CaH_2 to probe its high-pressure behaviour and also we perform first-principles calculations to aid the unambiguous assignment of the measured Raman vibrational modes and to understand better the physics behind the experimental observation. Indeed, a pressure-induced structural transition was identified at ∼15.5 GPa and the phase transition was found to complete at ∼21 GPa with a new phase being formed. The current exploration of CaH_2 also sheds strong light on the high-pressure behaviour of SrH_2 and BaH_2, as they share the same ground-state structure.

The high-pressure experiments for CaH_2 were carried out using a diamond anvil cell (DAC) with bevelled anvils with a 500 μm culet. A hole of 150 μm in diameter drilled in a pre-indented stainless-steel gasket with a thickness of 70 μm served as the sample chamber. CaH_2 (from Sigma Aldrich) of 99.9% purity and a modicum of ruby crystals of about 20 μm in size were loaded into the DAC in an inert atmosphere of nitrogen using a glove box equipped with a microscope because of the reactivity of the material. The pressure was calibrated on the basis of the fluorescence of the ruby [8]. For all the experiments, no pressure medium was used; since CaH_2 is very sensitive to moisture, it hydrolyzes readily with commonly used pressure-transmitting media like methanol/ethannol mixture or silicone oil. The pressure distribution was checked by measuring the fluorescence of ruby chips located at some points in the sample chamber. The maximum difference in the sample pressures was found to be less than ∼9% below 21.6 GPa. The small pressure distribution is expected, since CaH_2 is a very soft material and allows a fully relaxed sample during uploading of the pressure. Raman spectra were measured in a backscattering geometry using a Renishaw Raman microscope system. The spectral resolution was better than 2 cm^{-1}. Radiation with wavelengths of 514 nm from an argon-ion laser, 633 nm from a He–Ne laser and 830 nm from a semiconductor laser were used for excitation of the Raman spectra. The illuminated spot for the Raman measurements was less than 5 μm in size. All the spectra were measured at room temperature.

Ab initio lattice dynamic calculations were carried out using the plane-wave pseudopotential method within the linear response density functional theory through the Quantum-ESPRESSO package [9]. The generalized gradient approximation of the exchange–correlation functional [10, 11] is used. Particular attention was paid to generating a reliable hydrogen pseudopotential within the Troullier–Martins [12–14] norm-conserving scheme for the calculations at high pressures. A convergence test gave the choices of a 70 Ryd plane-wave cutoff and a $3 \times 6 \times 3$ Monkhorst-pack k mesh in the electronic Brillouin zone (BZ) integration. At selected pressure, the *Pnma* structure of CaH_2 (Ca and two inequivalant H atoms occupying Wyckoff 4c position) was fully optimized, allowing a variable cell and atomic positions. At zero pressure, the optimized lattice parameters a, b and c, and the atomic position x and z are listed in table 1 to compare with the experimental measurement for CaD_2 [15]. The excellent agreement between theory and experiment supports the validity of the current theoretical model.

The zone-centre (Γ) phonon frequencies, eigenvectors, and the dynamical matrix §(Γ) were thus calculated. The group theory analysis allows us to decompose the §(Γ) into blocks, each of them corresponding to an irreducible representation of the Γ-group. Therefore we can obtain irreducible representations of allowed Raman active phonons for the choice of structure.

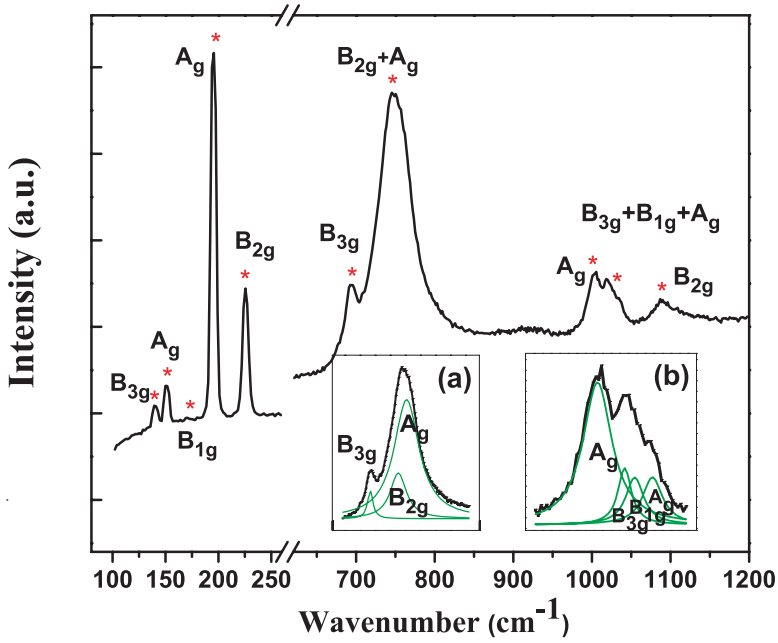

Figure 1. Raman spectra of CaH_2 measured under ambient conditions. The assignment of the experimentally observed Raman peaks (asterisk symbols) is based on the theoretical analysis. The insets (a) and (b) show the decompositions of the two broad Raman bands using the Lorentz function.

Table 1. The optimized structure parameters for CaH_2 at zero pressure. Experimental structure data for CaD_2 is also listed for comparison.

	Expt	Theory
a	5.92852(5)	5.9673
b	3.57774(3)	3.6062
c	6.78956(6)	6.8384
V	144.011(1)	147.156
Ca(x)	0.2387(1)	0.24
Ca(z)	0.1102(1)	0.1099
D1(x)	0.3558(1)	0.3557 (H1(x))
D1(z)	0.4276(1)	0.4265 (H1(z))
D2(x)	0.9750(1)	0.9754 (H2(x))
D2(z)	0.6756(1)	0.6765 (H2(z))

The CaH_2 crystallizes in an orthorhombic *Pnma* symmetry with 12 atoms in the unit cell. 33 optical modes are expected at the zone centre. Group theory analysis results in 18 Raman-active modes ($6A_g + 3B_{1g} + 6B_{2g} + 3B_{3g}$), 12 infrared-active modes ($5B_{1u} + 2B_{2u} + 5B_{3u}$), and three silent modes ($3A_u$).

Figure 1 shows our measured Raman spectrum at ambient pressure, together with the decompositions of the two broad Raman bands. It is found that at least nine Raman peaks (asterisk symbols) are clearly revealed. However, it is almost impossible to identify the vibrational modes without the help of theoretical analysis. Table 2 lists the comparison of our calculated and measured Raman mode frequencies. One observes that the overall agreement between theory and experimental is excellent by evidence of a largest deviation of 3.6% in the

Table 2. Comparison of the experimentally observed Raman mode frequencies with the first-principles results. The differences between theory and experiment (relative to the experimental values) are also presented for evaluation of the accuracy of both theory and experiment. All units are in cm^{-1}.

Modes	Expt (cm^{-1})	Theory (cm^{-1})	Deviation (%)
B_{3g}	139	137	1.4
A_g	150	147	2.0
B_{1g}	169	163	3.6
A_g	194	190	2.1
B_{2g}	224	223	0.4
B_{2g}		262	...
B_{1g}		663	...
A_g		672	...
B_{3g}	692	695	0.4
B_{2g}	738	715	3.1
A_g	753	754	0.1
B_{2g}		895	...
B_{2g}		976	...
A_g	1002	988	1.4
B_{3g}	1018	1022	0.4
B_{1g}	1024	1032	0.8
A_g	1034	1035	0.1
B_{2g}	1087	1090	0.3

low-frequency B_{1g} mode (169 cm^{-1}). The high accuracy in the theoretical calculation allows us to sign the Raman vibrational modes unambiguously, as shown in figure 1. Eigenvector analysis suggests that the strongest A_g Raman peaks centred at 194 cm^{-1} are attributed to Ca/diagonal motion within *a–c* plane. It is noteworthy that the very broad strong Raman peaks centred at 749 cm^{-1} consist of two Raman modes of B_{2g} (738 cm^{-1}) and A_g (753 cm^{-1}).

High-pressure *in situ* Raman scattering measurements were performed at up to 25.8 and 29.3 GPa for runs 1 and 2, respectively, with a Raman excitation of 514 nm from an argon-ion laser. The two measurements show practically similar pressure dependences on the Raman spectra, but run 2 with enough acquisition time gives a higher-resolution spectrum. Figure 2(a) shows the evolution of the Raman spectra with increasing pressure from run 2. It is found that there are several obvious changes in the Raman spectra with the application of pressure. Firstly, the Raman peak centred at 152 cm^{-1} (A_g) shows a blue-shift and increased peak intensity below 15.6 GPa. When the pressure goes beyond 15.6 GPa, the Raman peak position remains nearly unchanged and its intensity decreases until it disappears beyond 21.3 GPa. Secondly, the two Raman bands centred at 196 cm^{-1}(A_g) and 226 cm^{-1}(B_{2g}) move to higher energy and lose their intensities with pressure. Thirdly, on uploading pressure, the shoulder B_{3g} band (open symbols) at 708 cm^{-1} and the broad band ($B_{2g} + A_g$) at 752 cm^{-1} shift to higher energy and gain intensity under pressure below 14.5 GPa. However, the shoulder band moves faster, thus it merges into the nearby strong Raman band at 7.8 GPa. It is very interesting to note that at 14.5 GPa, the broad Raman band ($B_{2g} + A_g$) split into two bands, losing their intensities with a main peak softening and a shoulder peak hardening. Finally, it is very important to note that a new Raman peak (asterisk symbols) at 15.6 GPa centred at 212 cm^{-1} starts to appear and all the other Raman bands become weaker and weaker and eventually vanish. Beyond 21.3 GPa, only the new Raman band is visible in the energy range 100–1200 cm^{-1}. This Raman feature on uploading pressure clearly reveals a pressure-induced phase transition in CaH_2. The coexistence of the new and old Raman peaks suggests a mixed phase in the pressure range

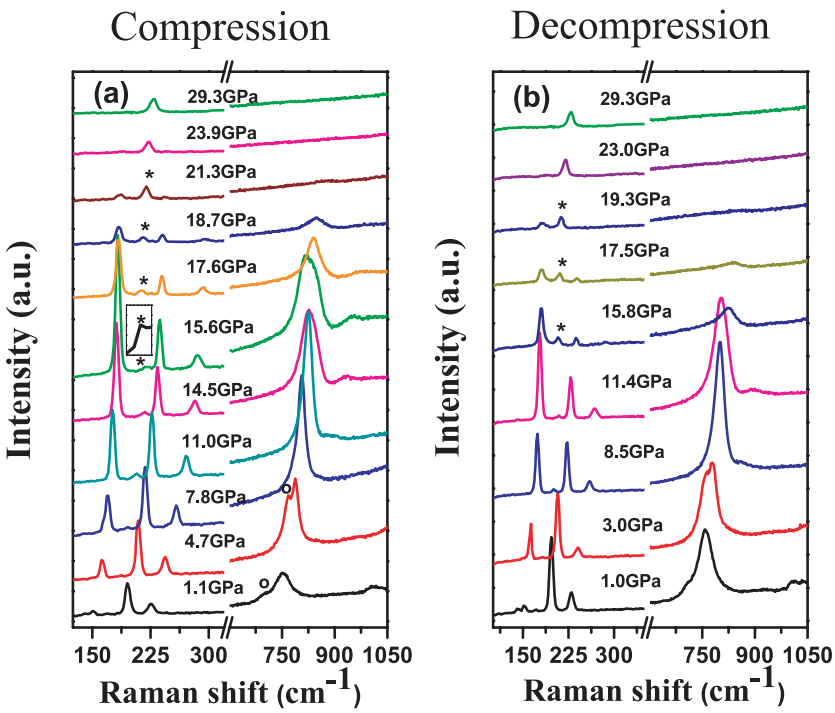

Figure 2. Raman spectra of CaH_2 as a function of pressure at room temperature for (a) compression and (b) decompression. The asterisks indicate the Raman peak corresponding to the new high-pressure phase, and the small inset in (a) at 15.6 GPa is a partial enlargement of the Raman spectrum to show clearly the appearance of the new Raman peak. The open symbol is an indication of the high-frequency shoulder peak of the A_g mode merging into the strong Raman peak with pressure.

15.6–21.3 GPa. During the process of downloading pressure, the spectrum gradually changes back to a pattern similar to that of the starting material (figure 2(b)). Thus a reversible phase transition is evidenced. However, the characteristic Raman mode for the new phase disappears at ∼12 GPa, which is much lower than the transition pressure of 15.6 GPa when uploading. This behaviour clearly suggests a hysteresis in the reversible transition.

Figure 3 shows the calculated and measured Raman shifts as a function of pressure. One observes that the theory and experiment is in excellent mutual agreement, especially for the three low-frequency modes. From the theoretical calculation of the high-frequency modes, we indeed found that the shoulder mode (violet open pentagon) in figure 2(a) shifts to higher energy faster than the main broad mode (orange open up triangle), resulting in a crossover between the two modes. Also, we predict a Raman mode (olive open circles) softening behaviour at 13.0 GPa. This mode softening might be attributable to the Raman softening behaviour in figure 2(a). It is noteworthy that this mode softening behaviour might be related to the physically driven force for the phase transition.

Another two independent high-pressure Raman measurements were also carried out with different Raman excitations of the 633 nm He–Ne laser and 830 nm solid-state laser. The phase transition pressures were identified at ∼15.5 and 16 GPa with highest loading pressures of up to 21.6 and 42.3 GPa, respectively. The slight difference in the transition pressure might be related to the non-hydrostatic effect. However, both of the experiment results reconfirmed the phase transition, and the highest pressure run demonstrates that the new high-pressure phase was

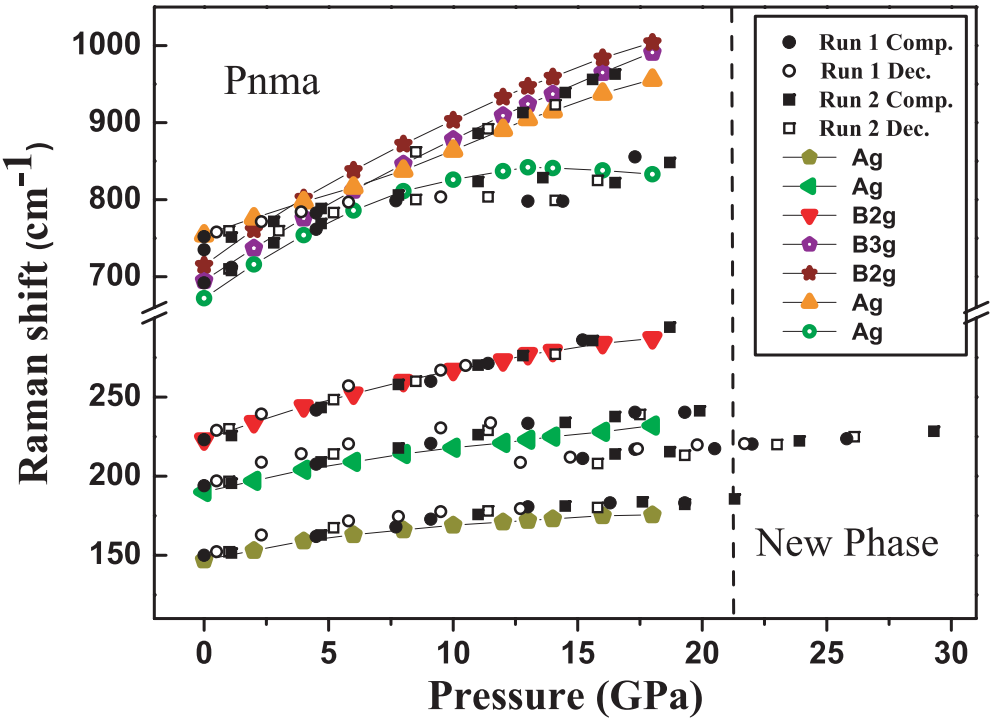

Figure 3. Pressure dependence of the measured (symbols) and simulated (symbols and lines) Raman modes for CaH_2. The solid and open circles (squares) are the measured data during the uploading and downloading processes for run 1 (run 2).

stable at least up to 42.3 GPa. Before we summarize, two implications should be addressed from the observation that there is only one Raman peak visible in the new phase of CaH_2. Firstly, it might suggest that the new phase possesses a higher symmetry with fewer atoms in the unit cell, which is necessary to reduce the number of optical branches at the zone centre. Secondly, in the formation of high-pressure incommensurate structures of solid bromine and iodine [16], seven Raman modes were reduced to only one low-frequency amplitude Raman mode for bromine ($\sim$80 cm^{-1}) and iodine ($\sim$40 cm^{-1}), respectively. Therefore, it is also possible for CaH_2 that an incommensurate structure was formed in which one amplitude Raman mode with low frequency ($\sim$210 cm^{-1}) was evidenced. However, for all the appearance, accurate neutron diffraction measurement is necessary to determine unambiguously the crystal structure of this novel high-pressure phase.

In conclusion, the vibrational properties of CaH_2 have been studied by *in situ* Raman scattering under high pressure. The results suggest that a pressure-induced phase transition occurred at about 15.5 GPa and completed at $\sim$21 GPa, and that this phase transition is reversible, with a hysteresis, to $\sim$12 GPa. The new high-pressure phase was found to be stable up to at least 42 GPa. First-principles calculations help to assign the measured Raman modes accurately and to understand the pressure dependence of the Raman frequency shift.

Acknowledgments

We thank the financial support of the China 973 Program under grant no. 2005CB724400, the NSAF of China under grant no. 10676011, the National Doctoral Foundation of China

Education Ministry under grant no. 20050183062, the Program for 2005 New Century Excellent Talents in University, and the 2006 Project for Scientific and Technical Development of Jilin Province.

Note added in proof. We noticed another experimental work on CaH_2 by Tse *et al*. Their measurements support the current finding.

References

[1] Schlapbach L and Zűttel A 2001 *Nature* **414** 353
[2] Fukai Y and Okuma N 1994 *Phys. Rev. Lett.* **73** 1640
[3] Chen Y and Williams J S 1995 *J. Alloys Compounds* **217** 181
[4] Zintl E and Harder A 1935 *Z. Elektrochem.* **43** 33
[5] Vajeeston P, Ravidran P, Kjekshus A and Fjellvåg H 2002 *Phys. Rev. Lett.* **89** 175506
[6] Vajeeston P, Ravindran P, Hauback B C, Fjellvåg H, Kjekshus A, Furuseth S and Hanfland M 2006 *Phys. Rev.* B **73** 224102
[7] Mao H K, Bell P M, Shaner J W and Steinberg D J 1978 *J. Appl. Phys.* **49** 3276
[8] Moriwaki T, Akahama Y, Kawamura H, Nakano S and Takemura K 2006 *J. Phys. Soc. Japan* **75** 074603
[9] Baroni S, Dal Corso A, de Gironcoli S, Giannozzi P, Cavazzoni C, Ballabio G, Scandolo S, Chiarotti G, Focher P, Pasquarello A, Laasonen K, Trave A, Car R, Marzari N and Kokalj A, http://www.pwscf.org/
[10] Perdew J P and Burke K 1996 *Int. J. Quantum Chem.* **S 57** 309
[11] Perdew J P, Burke K and Ernzerhof M 1996 *Phys. Rev. Lett.* **77** 3865
[12] Fuchs M and Scheffler M 1999 *Comput. Phys. Commun.* **119** 67
[13] Troulier N and Martins J L 1991 *Phys. Rev.* B **43** 1993
[14] Gonze X, Stumpf R and Scheffler M 1991 *Phys. Rev.* B **44** 8503
[15] Wu H, Zhou W, Udovic T J, Rush J J and Yildirim T 2006 Structure and vibrational spectra of calcium hydride and deuteride *J. Alloys Compounds* (doi:10.1016/j.jallcom.2006.07.042)
[16] Kume T, Hiraoka T, Ohya Y, Sasaki S and Shimizu H 2005 *Phys. Rev. Lett.* **94** 065506
[17] Tse J S, Klug D D, Desgreniers S, Smith J S, Flacau R, Liu Z, Hu J, Chen N and Jiang D T 2007 *Phys. Rev.* B at press